Mon. Not. R. Astron. Soc. **000**, 000,000 (2000)

Cosmic Statistics through Weak Lenses

Dipak Munshi[1⋆] and Peter Coles[2†]
[1] *Max-Planck-Institut fur Astrophysik, Karl-Schwarzschild-Str.1, D-85740, Garching, Germany*
[2] *School of Physics & Astronomy, University of Nottingham, University Park, Nottingham, NG7 2RD, United Kingdom*

25 March 2000

ABSTRACT
Many recent studies have demonstrated that scaling arguments, such as the so-called hierarchical *ansatz*, are extremely useful in understanding the statistical properties of weak gravitational lensing. This is especially true on small angular scales (i.e. at high resolution), where the usual perturbative calculations of matter clustering no longer apply. We build on these studies in order to develop a complete picture of weak lensing at small smoothing angles. In particular, we study the full probability distribution function, bias and other multipoint statistics for the "hot spots" of the convergence field induced by weak lensing, and relate these to the statistics of overdense regions in underlying mass distribution. It is already known that weak lensing can constrain the background geometry of the Universe, but we further show that it can also provide valuable information about the statistics of collapsed objects and the physics of collisionless clustering. Our results are particularly important for future observations which will, at least initially, focus on small smoothing angles.

Key words: Cosmology: theory – large-scale structure of the Universe – Methods: analytical – Methods: statistical

1 INTRODUCTION

The images of high redshift galaxies can be distorted by the gravitational lensing of light passing through intervening density fluctuations. Even the relatively weak lensing produced by large-scale galaxy clustering can provide valuable information about the distribution of mass on cosmological scales, as recent feasibility studies have demonstrated (Bacon, Refregier & Ellis 2000; van Waerbeke et al. 2000). Gravitational lensing studies offer a particular advantage over traditional studies of large-scale structure that rely on galaxies as tracers of mass. The analysis of galaxy catalogues can only provide us with information as to how galaxies are clustered, and galaxies need not be accurate tracers of the mass distribution, owing to the intervention of bias. To infer statistical properties of the underlying mass distribution from galaxy catalogues one needs to understand fully the relationship between mass and light, which is far from trivial to unravel. Weak lensing is produced by the mass distribution, and can therefore be used to probe the underlying mass distribution directly without having to allow for bias (Mellier 1999; Bernardeau 1999; Bartelmann & Schneider 1999).

After original suggestions by Gunn (1967), pioneering contributions on weak lensing were made by Blandford et al. (1991), Miralda-Escudé (1991), and Kaiser (1992). More recent developments basically follow two strands. Some authors have focussed on the case where large smoothing angles are used. In this regime highly non-linear effects are washed out, allowing simpler linear and quasi-linear analyses to be performed (Villumsen 1996; Stebbins 1996; Bernardeau et al. 1997; Kaiser 1998). A perturbative analysis can not be used to study lensing at small angular scales because the perturbation series begins to diverge as this limit is approached. The other approach that has been taken has involved the development of numerical experiments, usually using ray-tracing methods through N-body simulations (Schneider & Weiss 1988; Jarosszn'ski et al. 1990; Lee & Paczyn'ski 1990; Jarosszn'ski 1991; Babul & Lee 1991; Bartelmann & Schneider 1991; Blandford et al. 1991). Building on the earlier work of Wambsganns et al. (1995, 1997, 1998) the most detailed numerical study of lensing so far was performed by Wambsganns, Cen & Ostriker (1998). Other recent studies involving ray-tracing experiments have been conducted by Premadi, Martel & Matzner (1998), van Waerbeke, Bernardeau & Mellier (1998), Bartelmann et al. (1998) and Couchman, Barber & Thomas (1998).

⋆ e-mail: mdipak@mpa-garching.mpg.de
† e-mail: Peter.Coles@nottingham.ac.uk

A complete statistical analysis of weak lensing on small angular scales is not available at present, cheifly because no corresponding analysis exists for the underlying density field. There are, however, several non-linear *ansatze* available. These predict a tree hierarchy for the matter correlation functions and are successful in some respects at modelling the results from numerical simulations of gravitational clustering (Davis & Peebles 1977; Peebles 1980; Fry 1984; Fry & Peebles 1978; Szapudi & Szalay 1993, 1997; Scoccimarro & Frieman 1998; Scoccimarro et al. 1998). The different *ansatze* involved in these studies all involve a tree hierarchy, but disagree with each other in the way they assign weights to trees of same order but different topology (Balian & Schaeffer 1989; Bernardeau & Schaeffer 1992; Szapudi & Szalay 1993; Boschan, Szapudi & Szalay 1994). The overall scaling in such models, determined by the time evolution of the two-point correlation function, is left arbitrary. However recent studies by several authors (Hamilton et al 1991, Nityananda & Padmanabhan 1994, Jain, Mo & White 1995; Padmanabhan et al. 1996; Peacock & Dodds 1996) have furnished an accurate fitting formula for the evolution of the two-point correlation function which can be used in combination with the hierarchical *ansatze* to predict all clustering properties of the dark matter distribution in the universe.

The statistical treatments of lensing that have been carried out so far have mainly concentrated on the properties of low-order cumulants (van Waerbeke, Bernardeau & Mellier 1998; Schneider et al. 1998; Hui 1999; Munshi & Coles 2000; Munshi & Jain 1999a), cumulant correlators (Munshi & Jain 1999b) and errors associated with their measurement from observational data (Reblinsky et al. 1999; Schneider et al. 1998). However it is well known that higher and higher order moments are more and more sensitive to the tail of the distribution from which they are derived represent and are also more sensitive to errors due to finite catalogue size (Colombi et al. 1995; Colombi et al. 1996; Szapudi & Colombi 1996; Hui & Gaztanaga 1998). On the other hand, numerical simulations involving ray tracing techniques have demonstrated that the distribution of lensed fluctuations can be of considerable assistance in the estimation of cosmological parameters from observational data (Jain & Seljak 1997; Jain, Seljak & White 1999; Jain & Van Waerbeke 1999). The probability distribution function associated with density field is not sensitive to cosmological parameters in the way its weakly-lensed counterpart is.

Munshi & Jain (1999a,b) and Munshi (2000) have extended these studies to show that the hierarchical *ansatz* can actually be used to make concrete analytical predictions for all statistical properties of the convergence that results from weak lensing. Valageas (1999a) has also used the hierarchical *ansatz* to compute the error involved in estimating the cosmological parameters Ω_0 and Λ_0 from supernova observations; see alo Wang (1999). In Valageas (1999b) the effect of smoothing was incorporated successfully to compute the PDF of the convergence field.

In this paper we extend these analyses still further to develop a complete picture of statistical properties of the sky-projected density field obtained by weak-lensing surveys. In particular, we obtain an analytic prediction for probability distribution function (PDF), bias and higher-order moments for regions where the projected density is particularly high. We also show how these the statistics of these 'hotspots' are related to similar quantities in the underlying mass distribution. These results can be used to understand the effect of changing source redshift, smoothing angle and cosmological parameters such as Ω_0 and Λ_0. This will allow a more detailed exploration of cosmological parameter space than is possible with ray-tracing experiments. Several of the analytic results we discuss here have already been tested against high resolution numerical simulations and found to be in very good agreement. Finally, we will also show that our present understanding of gravitational clustering is sufficient to make firm predictions that can be tested using future observations.

Throughout this analysis we will be neglecting noise due to source ellipticity and will also be neglecting source clustering. A complete error analysis of different statistics with these contributions taken into account will be presented elsewhere (Munshi & Coles 2000b).

The paper is organized as follows. In Section 2 we present a detailed analysis of the PDF for smoothed convergence field κ_s. In Section 2 we present an analysis of the bias associated with peaks in smoothed convergence field κ_s. Sections 4-6 are devoted to the study of third-, fourth-, and fifth-order statistics (respectively) of the smoothed convergence field. In Section 7 we generalize these results to arbitrary order and in section 8 we comment about our results in general cosmological setting.

2 THE DENSITY PDF FROM CONVERGENCE MAPS

Our formalism is based on a hierarchical *ansatz* for the matter correlation functions. In principle the entire set of N-point correlation functions must be computed by solving a coupled series of non-linear integro-differential equations known as BBGKY hierarchy. Unfortunately, no such solution exists at present. On the other hand, the Vlasov-Poisson system in the fluid limit does admit hierarchical scaling solutions. Motivated by this fact, several well-known hierarchical *ansatze* have been suggested which are very helpful in understanding the non-linear dynamics of gravitational clustering. One of these *ansatz* is particularly interesting, namely the one proposed by Balian & Schaeffer (1989) and developed considerably by Bernardeau & Schaeffer (1992). These studies are based on multi-point cell count statistics and their scaling properties. To apply it to lensing statistics is reasonably straightforward in principle, but requires some preliminaries.

We adopt the following line element to describe the background geometry:

$$d\tau^2 = -c^2dt^2 + a^2(t)(d\chi^2 + r^2(\chi)d^2\Omega), \tag{1}$$

where $a(t)$ is the expansion factor. The angular diameter distance $r(\chi) = K^{-1/2}\sin[K^{-1/2}\chi]$ for positive spatial curvature, $r(\chi) = (-K)^{-1/2}\sinh[(-K)^{-1/2}\chi]$ for negative curvature, and $r(\chi) = \chi$ for a flat universe. In terms of H_0 and Ω_0, $K = (\Omega_0 - 1)H_0^2$.

We shall focus on the properties of the convergence $\kappa(\gamma)$ produced by lensing. In the standard terminology of gravitational

lensing this is simply the ratio of the surface mass density $\Sigma(\gamma)$ (observed in a direction γ to the critical surface density for lensing $\Sigma_{\rm cr}$. In our background geometry this reduces to a weighted integral of the density fluctuation $\delta(\mathbf{x})$ along the line of sight:

$$\kappa(\gamma) = \int_0^{\chi_s} d\chi \omega(\chi) \delta\left[r(\chi), \gamma\right]. \tag{2}$$

If all the sources are at the same redshift, one can express the weight function $\omega(\chi) = 3/4ac^{-2}H_0^2\Omega_m r(\chi)r(\chi_s - \chi)/r(\chi_s)$, where χ_s is the comoving radial distance to the source. (This approximation is not essential to the calculation, and it is easy to modify what follows for a more accurate description.) Using the definitions we have introduced above we can compute the projected variance of κ in terms of the power spectrum of density fluctuations $P(\mathbf{l})$ using

$$\langle \kappa_s^2 \rangle = \int_0^{\chi_s} d\chi_1 \frac{\omega^2(\chi_1)}{r^2(\chi_1)} \int \frac{d^2\mathbf{l}}{(2\pi)^2}\, P\left(\frac{\mathbf{l}}{r(\chi)}\right) W^2(l\theta_0), \tag{3}$$

(Limber 1954). The higher order moments of the convergence field can be written in the form:

$$\langle \kappa_s^N \rangle = S_N \int_0^{\chi_s} d\chi \frac{\omega^N(\chi)}{r^{2(N-1)}(\chi)} \kappa_{\theta_0}^{N-1}, \tag{4}$$

(Munshi & Coles 2000a), where the S_N are defined by analogy with the hierarchical parameters usually used in the context of galaxy counts-in-cells.

If the mean number of galaxies per cell is $\bar{N}$ and the volume-average of the two-point correlation function over the cell is

$$\bar{\xi}_2 = \frac{1}{V^2} \int \int \xi_2(\mathbf{r}_1, \mathbf{r}_2) dV_1 dV_2, \tag{5}$$

then the generalisation of equation the previous equation

$$\bar{\xi}_N = \frac{1}{V^N} \int \ldots \int \xi_N(\mathbf{r}_1 \ldots \mathbf{r_N}) dV_1 \ldots dV_N. \tag{6}$$

leads to the description of higher-order statistical properties of galaxy counts in terms of the scaling parameters S_N constructed from the $\bar{\xi}_N$ via

$$S_N = \frac{\bar{\xi}_N}{\bar{\xi}_2^{N-1}}. \tag{7}$$

In equation (4) we have also introduced a new notation, namely that

$$\kappa_{\theta_0} = \int \frac{d^2\mathbf{l}}{(2\pi)^2} P\left(\frac{l}{r(\chi)}\right) W^2(l\theta_0), \tag{8}$$

in order to take account of smoothing over an angular scale θ_0. The function $W(l\theta_0)$ is the window function for the smoothing. In many studies a top-hat filter is used for smoothing the convergence field, but our study can be extended to compensated filters (Schneider et al. 1998; Reblinsky et al. 1999), which may be more appropriate for observational purposes.

In order to compute the PDF of the smoothed convergence field κ_s, we will begin by constructing its associated cumulant generating function $\Phi^{1+\kappa}(y)$

$$\Phi^{1+\kappa}(y) = y + \sum_{p=2}^{\infty} \frac{\langle \kappa_s^p \rangle}{\langle \kappa_s \rangle^{p-1}} y^p. \tag{9}$$

Using the expression for the higher moments of the convergence field κ_s we can write

$$\Phi^{1+\kappa}(y) = y + \int_0^{\chi_s} \sum_{N=2}^{\infty} \frac{(-1)^N}{N!} S_N \frac{\omega^N(\chi)}{r^{2(N-1)}(\chi)} \kappa_{\theta_0}^{(N-1)} \frac{y^N}{\langle \kappa_s^2 \rangle^{(N-1)}}. \tag{10}$$

We can now express $\Phi^{1+\kappa}(y)$, in terms of the cumulant generating function of the matter distribution, $\phi(y)$ using

$$\phi(y) = \sum_{p=1}^{\infty} \frac{S_P}{p!} y^p, \tag{11}$$

in which the constants S_p are the0 hierarchical parameters discussed above. In terms of $\phi^\eta(y)$ we get

$$\Phi^{1+\kappa}(y) = \int_0^{\chi_s} r^2(\chi) d\chi \left[\frac{\kappa_{\theta_0}}{\langle \kappa_s^2 \rangle}\right]^{-1} \phi^\eta\left[y \frac{\omega(\chi)}{r^2(\chi)} \frac{\kappa_{\theta_0}}{\langle \kappa_s^2 \rangle}\right] - y \int_0^{\chi_s} \omega(\chi) d\chi. \tag{12}$$

The second term in eq. (12) comes from the $N = 1$ term in the expansion of $\Phi^{1+\kappa}$. Note that we have used the fully non-linear generating function ϕ^η for the cumulants, though we will use it to construct a generating function in the quasi-linear regime.

The analysis simplifies if we define a new reduced convergence field η_s defined by

$$\eta_s = \frac{\kappa_s - \kappa_m}{-\kappa_m} = 1 + \frac{\kappa_s}{|\kappa_m|}, \tag{13}$$

where the minimum value of κ_s, denoted κ_m, occurs when the line of sight goes through regions that are completely devoid of matter (i.e. $\delta = -1$ all along the line of sight):

$$\kappa_m = -\int_0^{\chi_s} d\chi \omega(\chi). \tag{14}$$

Although $\kappa(\theta_0)$ depends on the smoothing angle, its minimum value κ_m depends only on the source redshift and background geometry of the universe and is independent of the smoothing radius. In terms of the reduced convergence η_s, the cumulant generating function is given by,

$$\Phi^\eta(y) = \frac{1}{[\kappa_m]^2} \int_0^{\chi_s} r^2(\chi) d\chi \Big[\frac{\kappa_{\theta_0}}{\langle\kappa_s^2\rangle}\Big]^{-1} \phi^\eta\Big[y\kappa_m \frac{\omega(\chi)}{r^2(\chi)} \frac{\kappa_{\theta_0}}{\langle\kappa_s^2\rangle}\Big] \tag{15}$$

The new cumulant generating function $\Phi^\eta(y)$ satisfies the normalization constraints $S_1 = S_2 = 1$.

The scaling function associated with $P^\eta(\eta)$ can now be related to the matter scaling function $h(x)$ introduced in Munshi et al. (1999a) in the context of matter clustering. This function is defined in terms of the scaling variable $x = N/N_c$, where $N_c = \bar{N}\bar{\xi}_2$. In the hierarchical *ansatz* the probability distribution $P(N)$ can be expressed in scaled form as

$$P(N) = \frac{1}{\bar{\xi}_2 N_c} h(x). \tag{16}$$

The quantity $h(x)$ can then be expressed in terms of an integral of the form

$$h(x) = -\frac{1}{2\pi i} \int_{i\infty}^{i\infty} dy\ y\sigma(y) \exp(yx). \tag{17}$$

This can be extended to the bias factor of cells of occupancy N via

$$P(N)b(N) = \frac{1}{\xi_2 N_c} h(x)b(x) \tag{18}$$

and so on for higher-order statistics; see Munshi et al. (1999a) for more details.

In the present context we instead define

$$H^\eta(x) = -\int_{-\infty}^{\infty} \frac{dy}{2\pi i} \exp(xy)\Phi^\eta(y). \tag{19}$$

Using this definition we can write

$$H^\eta(x) = \frac{1}{\kappa_m} \int_0^{\chi_s} \omega(\chi) d\chi \Big[\frac{r^2(\chi)\langle\kappa_s^2\rangle}{\omega(\chi)\kappa_{\theta_0}\kappa_m}\Big]^2 h^\eta\left[\frac{\langle\kappa_s^2\rangle}{\kappa_{\theta_0}} \frac{r^2(\chi)}{\omega(\chi)} \frac{x}{\kappa_m}\right]. \tag{20}$$

These equations apply to the most general case within the small angle approximation, but can be simplified considerably using further approximations. In the following we will assume that the contribution to the integrals involved in the expressions for χ can be replaced by an average value coming from the maximum of $\omega(\chi)$, i.e. χ_c $(0 < \chi_c < \chi_s)$. This idea leads to the following approximate expressions:

$$\begin{aligned} |\kappa_m| &\approx \frac{1}{2}\chi_s \omega(\chi_c) \\ \langle\kappa_s^2\rangle &\approx \frac{1}{2}\chi_s \omega^2(\chi_c)\Big[\frac{d^2k}{(2\pi)^2}\mathrm{P(k)}W^2(kr(\chi_c)\theta_0)\Big]. \end{aligned} \tag{21}$$

Using these approximations we can write

$$\begin{aligned} \Phi^\eta(y) &= \phi^\eta(y) \\ H^\eta(x) &= h^\eta(x). \end{aligned} \tag{22}$$

We thus find that the statistics of the smoothed underlying field and those of the reduced convergence η are exactly the same in this approximation. (The approximate functions Φ^η and $h^\eta(x)$ do satisfy the correct normalization constraints, but we omit the details here.)

Although it is possible to integrate the exact expressions of the scaling functions, there is some uncertainty involved in the actual determination of these functions and their associated parameters which must be inferred from numerical simulations. See Colombi et al. (1996), Munshi et al. (1999a) and Valageas et al. (1999) for a detailed description of the effect of finite volume corrections involved in their estimation. In numerical studies involving ray tracing simulations (Munshi & Jain 1999b) it has been found that the minimal hierarchical model of Bernardeau & Schaeffer (1992), which has only one free parameter to be determined from numerical simulations, can reproduce results from simulations very accurately.

Another useful approach is to construct an Edgeworth expansion of the PDF, starting with the simpler form $P(\eta_s)$. This can then be used to construct a series for $P(\kappa_s)$. The Edgeworth expansion (Bernardeau & Kofman 1994) is meaningful when

the variance is less than unity, a condition that guarantees a convergent series expansion in terms of Hermite polynomials $H_n(\nu)$, of order n and with $\nu = \eta_s/\sqrt{(\xi_{\eta_s})}$.The relevant series expansion is

$$P^{\eta}(\eta_s) = \frac{1}{\sqrt{2}\pi\bar{\xi}_{\eta_s}} \exp(-\frac{\nu^2}{2}) \Big[1 + \sqrt{\bar{\xi}}_{\eta} \frac{S_3^{\eta}}{6} H_3(\nu) + \sqrt{\bar{\xi}}_{\eta}^{\,2} \Big(\frac{S_4^{\eta}}{24} H_4(\nu) + \frac{S_3^{\eta\,2}}{72} H_6(\nu) \Big) + \dots \Big] \tag{23}$$

This is usually applied to a quasi-linear analysis of matter clustering using perturbative expressions for the cumulants. However, the S_N^{η} parameters needed in the expansion of $P(\eta)$ are from the highly non-linear regime. Although the variance is still smaller than unity, the parameters that characterize it emerge from the highly non-linear dynamics of the underlying dark matter distribution.

The magnification μ can also be used instead of κ according to the weak lensing relation, $\mu_s = 1 + 2\kappa_s$. Its minimum value can be related to κ_m defined earlier via $\mu_m = 1 + 2\kappa_m$. Finally, the reduced convergence η and the magnification μ can be related by the following equation:

$$\eta_s = \frac{\mu_s - \mu_m}{1 - \mu_m} \tag{24}$$

(Valageas 1999). We can now express the relations connecting the probability distribution function for the smoothed convergence statistics κ_s, the reduced convergence η_s and the magnification μ_s as,

$$P^{\kappa}(\kappa_s) = 2P^{\mu}(\mu_s) = P^{\eta}(\eta_s)\frac{2}{(1-\mu_m)} = P^{\eta}(\eta_s)\frac{1}{|\kappa_m|}. \tag{25}$$

The formalism which we have developed for one-point statistics such as the PDF and the VPF can also be extended to compute the bias and higher order cumulants associated with spots in κ maps above a certain threshold. The statistics of such spots can be associated with the statistics of over-dense regions in the underlying mass distribution representing the collapsed objects. A detailed analysis of these issues will be presented elsewhere (Munshi & Coles 2000b).

3 BIAS OF COLLAPSED OBJECTS FROM CONVERGENCE MAPS

In order To compute the bias associated with the peaks in the convergence field we must first develop an analytic expression for the joint generating function $\beta(y_1, y_2)$ for the convergence field κ_s. For that we will use the usual definition for the two-point cumulant correlator C_{pq} of the convergence field

$$C_{pq}^{\kappa} = \frac{\langle \kappa_s(\gamma_1)^p \kappa_s(\gamma_2)^q \rangle}{\langle k_s^2 \rangle^{p+q-2} \langle \kappa_s(\gamma_1)\kappa_s(\gamma_2) \rangle} = C_{p1}^{\kappa} C_{q1}^{\kappa}. \tag{26}$$

For a complete treatment of lower order moments of κ_s, see Munshi & Coles (2000a). Like its counterpart for the density field, the two-point generating function of the convergence field can be expressed as a product of two one-point generating functions:

$${}_2\beta_{\kappa}(y_1, y_2) = \sum_{p,q}^{\infty} \frac{C_{pq}^{\kappa}}{p!q!} y_1^p y_2^q = \sum_{p}^{\infty} \frac{C_{p1}^{\kappa}}{p!} y_1^p \sum_{q}^{\infty} \frac{C_{q1}^{\kappa}}{q!} y_2^q = \beta_{\kappa}(y_1)\beta_{\kappa}(y_2) \equiv \tau_{\kappa}(y_1)\tau_{\kappa}(y_2), \tag{27}$$

where the function τ_{κ} will be used later. The factorization property of the generating function depends on the factorization property of the cumulant correlators: $C_{pq}^{\eta} = C_{p1}^{\eta} C_{q1}^{\eta}$. Such a factorization is possible when the correlation between two patches in the directions γ_1 and γ_2 is smaller than the variance on the scale of one patch. Using this and starting with

$${}_2\beta_{\kappa}(y_1, y_2) = \sum_{p,q}^{\infty} \frac{1}{p!q!} \frac{y_1^p y_2^q}{\langle \kappa_s^2 \rangle^{p+q-2}} \frac{\langle \kappa_s(\gamma_1)^p \kappa_s(\gamma_2)^q \rangle}{\langle \kappa_s(\gamma_1)\kappa_s(\gamma_2) \rangle}, \tag{28}$$

and then inserting the integral expression for the cumulant correlators in the hierarchical *ansatz* we obtain

$${}_2\beta_{\kappa}(y_1, y_2) = \sum_{p,q}^{\infty} \frac{C_{pq}^{\eta}}{p!q!} \frac{1}{\langle \kappa_s^2 \rangle^{p+q-2}} \frac{1}{\langle \kappa_s(\gamma_1)\kappa_s(\gamma_2) \rangle} \int_0^{\chi_s} d\chi \frac{\omega^{p+q}}{r^{2(p+q-1)}} \kappa_{\theta_{12}} \kappa_{\theta_0}^{p+q-2} y_1^p y_2^q. \tag{29}$$

This expression involves the definition

$$\kappa_{\theta_{12}} = \int \frac{d^2\mathbf{l}}{(2\pi)^2} P\left(\frac{l}{r(\chi)}\right) W^2(l\theta_0) \exp(il\theta_{12}). \tag{30}$$

It is possible to simplify this approximation further by grouping the summations over dummy variables p and q. This is useful to establish the factorization property of the two-point (joint) generating function for bias ${}_2\beta(y_1, y_2)$. Note that

$${}_2\beta_{\kappa}(y_1, y_2) = \int_0^{\chi_s} r^2(\chi) d\chi \left[\frac{\kappa_{\theta_{12}}}{\langle \kappa_s(\gamma_1)\kappa_s(\gamma_2) \rangle}\right] \left[\frac{\kappa_{\theta_0}}{\langle \kappa_s^2 \rangle}\right]^{-2} \sum_{pq}^{\infty} \frac{C_{pq}^{\eta}}{p!q!} \left[y_1 \frac{\omega(\chi)}{r^2(\chi)} \frac{\kappa_{\theta_0}}{\langle \kappa_s^2 \rangle}\right]^p \left[y_2 \frac{\omega(\chi)}{r^2(\chi)} \frac{\kappa_{\theta_0}}{\langle \kappa_s^2 \rangle}\right]^q. \tag{31}$$

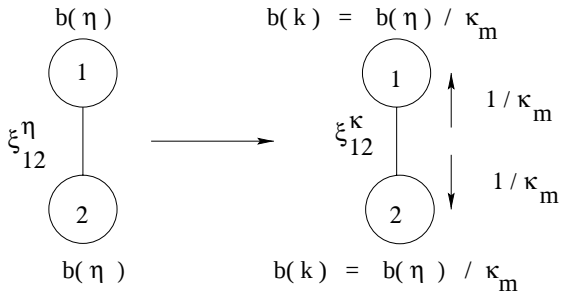

Figure 1. Construction of bias function $b(\kappa_s)$ for the smoothed convergence field from the bias $b(\eta_s)$ associated with the smoothed reduced convergence field η_s.

We can now decompose the double sum over the two indices into two separate sums over individual indices. Finally using the definition of the one-point generating function for the cumulant correlators we can write:

$$ {}_2\beta_\kappa(y_1, y_2) \quad = \quad \int_0^{\chi_s} r^2(\chi) d\chi \left[\frac{\kappa_{\theta_{12}}}{\langle \kappa_s(\gamma_1)\kappa_s(\gamma_2)\rangle}\right] \left[\frac{\kappa_{\theta_0}}{\langle \kappa_s^2\rangle}\right]^{-2} \tau^\eta \left[y_1 \frac{\omega(\chi)}{r^2(\chi)} \frac{\kappa_{\theta_0}}{\langle \kappa_s^2\rangle}\right] \tau^\eta \left[y_2 \frac{\omega(\chi)}{r^2(\chi)} \frac{\kappa_{\theta_0}}{\langle \kappa_s^2\rangle}\right] \tag{32} $$

The above expression is quite general. It depends on the small-angle and large separation approximations, but is valid for any particular model for the tree-correlation hierarchy. However it can be seen that the projection effects encoded in the line-of-sight integration do not allow us to express the two-point generating function $\beta_\eta(y_1, y_2)$ simply as a product of two one-point generating functions $\beta^\eta(y)$ as can be done in the case of the underlying density field.

As in the case of the derivation of the probability distribution function for the smoothed convergence field κ_s, matters simplfy considerably if we use the reduced smoothed convergence field η_s. We have already shown that the PDF associated with η_s and the underlying mass distribution are the same under certain approximations. An identical ressult result indeed holds good for higher order statistics, including the bias. The cosmological dependence of the statistics of κ_s field is encoded in k_m and the choice of the new variable η renders its related statistics almost independent of background cosmology. Repeating the above analysis again for the η_s field now we can express the cumulant correlator generating function for the reduced convergence field η_s as follows:

$$ {}_2\beta_\eta(y_1, y_2) = \frac{1}{[\kappa_m]^2} \int_0^{\chi_s} r^2(\chi) d\chi \left[\frac{\kappa_{\theta_{12}}}{\langle \kappa_s(\gamma_1)\kappa_s(\gamma_2)\rangle}\right] \left[\frac{\kappa_{\theta_0}}{\langle \kappa_s^2\rangle}\right]^{-2} \tau^\eta \left[y_1 \kappa_m \frac{\omega(\chi)}{r^2(\chi)} \frac{\kappa_{\theta_0}}{\langle \kappa_s^2\rangle}\right] \tau^\eta \left[y_2 \kappa_m \frac{\omega(\chi)}{r^2(\chi)} \frac{\kappa_{\theta_0}}{\langle \kappa_s^2\rangle}\right]. \tag{33} $$

Although the above expression is very accurate and describes an important relationship between the density field and the convergence field, it is difficult to use for any practical purpose. It is also important to note that scaling functions such as $h(x)$ for the density probability distribution function and $b(x)$ for the bias associated with over-dense objects are typically estimated from numerical simulations, especially in the highly non-linear regime. Such estimations are subject to many uncertainties, such as the finite size of the simulation box. It has been noted in earlier studies that such uncertainties lead to large errors in estimates of $h(x)$. Estimates of the scaling function associated with the bias $b(x)$ is even more complicated, owing to the fact that these quantities are even worse affected finite size of the catalogues. It is consequently not fruitful to integrate the exact integral expression we have derived above. Instead we will replace all line-of-sight integrals with approximate values. An exactly similar approximation was used by Munshi & Jain (1999a) to simplify the one-point probability distribution function for κ_s, and it was found to be in good agreement with numerical simulations. In this approximation

$$ \langle \kappa_s(\gamma_1)\kappa_s(\gamma_2)\rangle \approx \frac{1}{2}\chi_s \omega^2(\chi_c) \Big[\frac{d^2k}{(2\pi)^2} \mathrm{P(k)} W^2(kr(\chi_c)\theta_0) \exp[ikr(\chi_c)\theta_{12}]\Big]. \tag{34} $$

This gives us the leading order contributions to the integrals needed and we can also check that, to this order, we recover the factorization property of the generating function, i.e.

$$ {}_2\beta_\eta(y_1, y_2) = \tau^\eta(y_1)\tau^\eta(y_2) = \tau_{1+\delta}(y_1)\tau_{1+\delta}(y_2) \equiv \tau(y_1)\tau(y_2). \tag{35} $$

It is also interesting to note that $C^\kappa_{p1} = C^\eta_{p1} {\kappa_m}^{p-1}$.

In this level of approximation, the factorization property of the cumulant correlators means that the bias function $b(x)$ associated with the peaks above a given threshold in the convergence field κ_s also obey a factorization property, just as is the case in the density field counterpart (e.g. Coles, Munshi & Melott 2000):

$$ b^\eta(x_1)h^\eta(x_1)b^\eta(x_2)h^\eta(x_2) = b_{1+\delta}(x_1)h_{1+\delta}(x_1)b_{1+\delta}(x_2)h_{1+\delta}(x_2), \tag{36} $$

in which we have used the relation between $\beta(y)$ and $b(x)$ given above:

$$ b^\eta(x)h^\eta(x) = -\frac{1}{2\pi i} \int_{-i\infty}^{i\infty} dy \tau(y) \exp(xy). \tag{37} $$

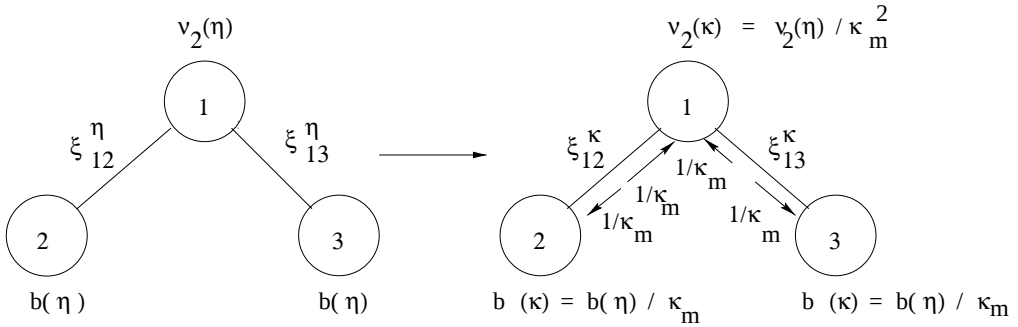

Figure 2. Construction of the bias function $b(\kappa_s)$ for the smoothed convergence field from the bias $b(\eta_s)$ associated with the smoothed reduced convergence field η_s.

We established a similar correspondence between the convergence field and density field in the case of one-point probability distribution function in the previous section.

The differential bias, i.e. the bias associated with a particular overdensity, is much more difficult to measure from numerical simulations than its integral counterpart. From now on we therefore concentrate on the bias associated with peaks above certain threshold, which can be expressed in a similar form to that given above:

$$b^{\eta}(>x)h^{\eta}(>x) = -\frac{1}{2\pi i}\int_{-i\infty}^{i\infty} dy \frac{\tau(y)}{y}\exp(xy). \tag{38}$$

(Munshi et al. 1999a). Although the bias $b(x)$ associated with the convergence field and that related to the underlying density field are exactly equal, the variance associated with the density field is very much higher than that of the convergence field. Projection effects bring down the latter to less than unity, meaning that we have to use the integral definition of bias to recover it from its generating function (see eq.(37) and eq.(38)).

We can now write down the full two-point probability distribution function for two correlated spots in terms of the convergence field κ and its reduced version η:

$$\begin{aligned} p^{\kappa}(\kappa_1,\kappa_2)d\kappa_1 d\kappa_2 &= p^{\kappa}(\kappa_1)p^{\kappa}(\kappa_2)\left[1+b^{\kappa}(\kappa_1)\xi^{\kappa}_{12}b^{\kappa}(\kappa_2)\right]d\kappa_1 d\kappa_2 \\ p^{\eta}(\eta_1,\eta_2)d\eta_1 d\eta_2 &= p^{\eta}(\eta_1)p^{\eta}(\eta_2)\left[1+b^{\eta}(\eta_1)\xi^{\eta}_{12}b^{\eta}(\eta_2)\right]d\eta_1 d\eta_2. \end{aligned} \tag{39}$$

Following from the analysis presented in the previous section, we note that $p(\kappa_s) = p(\eta_s)/k_m$ and that $\xi^{\kappa}_{12} = \xi^{\eta}_{12}/\kappa^2_m$. Using these relations we can now write

$$b^{\kappa}(\kappa) = \frac{b^{\eta}(\eta)}{k_m}. \tag{40}$$

This is one of the main results of this analysis and has already been shown by Munshi (2000) to be in very good agreement with numerical ray tracing simulations.

4 THREE-POINT STATISTICS OF COLLAPSED OBJECTS FROM CONVERGENCE MAPS

A non-linear *ansatz* for higher-order correlations can be used not only to compute the correlation hierarchy for the underlying mass distribution but also the multi-point statistics of overdense cells, which represent collapsed objects (Bernardeau & Schaeffer 1992, 1999; Munshi et al. 199a,b,c; Coles et al. 1999). Whereas such studies generally concentrate mainly on three-dimensional statistical properties our aim in this paper is to investigate how much one can learn from such *ansatze* about the projected density field obtained from weak lensing surveys. In earlier sections we showed that the bias associated with peaks in projected density field can be very accurately modelled. We will now extend these results using multi-point cumulant correlators to show that such an analysis can also be performed for the skewness of overdense objects in the projected density field.

The bias of collapsed objects is connected with the two-point cumulant correlators of the underlying mass distribution. In a very similar fashion, the three-point cumulant correlators of underlying mass distribution can be related to the skewness of collapsed objects. The three-point cumulant correlators for projected mass distribution, smoothed with an angle θ_0 can be written as (Munshi & Coles 2000a)

$$\langle\kappa_s(\gamma_1)^p\kappa_s(\gamma_2)^q\kappa_s(\gamma_3)^r\rangle_c = \int_0^{\chi_s} d\chi \frac{\omega^{p+q+r}}{r^{2(p+q+r-1)}}\left[C^{\eta}_{p1}\kappa_{\theta_{12}}C^{\eta}_{q11}\kappa_{\theta_{23}}C^{\eta}_{r1}\kappa^{p+q+r-3}_{\theta_0} + \quad \text{cyc.perm.}\right]. \tag{41}$$

The three-point cumulant correlators for the projected density field can be defined by the following equation:

$$C^{\kappa}_{pqr} = \frac{\langle\kappa_s(\gamma_1)^p\kappa_s(\gamma_2)^q\kappa_s(\gamma_3)^r\rangle_c}{\langle\kappa_s(\gamma_1)\kappa_s(\gamma_2)\rangle_c\langle\kappa_s(\gamma_2)\kappa_s(\gamma_3)\rangle_c\langle\kappa^2(\gamma)\rangle_c^{p+q+r-3}}$$

$$= \int_0^{\chi_s} d\chi \frac{\omega^{p+q+r}}{r^{2(p+q+r-1)}} C^{\eta}_{p1} \frac{\kappa_{\theta_{12}}}{\langle \kappa_s(\gamma_1)\kappa_s(\gamma_2)\rangle_c} C^{\eta}_{q11} \frac{\kappa_{\theta_{23}}}{\langle \kappa_s(\gamma_2)\kappa_s(\gamma_3)\rangle_c} C^{\eta}_{r1} \frac{\kappa^{(p+q+r-3)}_{\theta_0}}{\langle \kappa^2_s(\gamma)\rangle^{(p+q+r-3)}_c}. \quad (42)$$

In what follows we present only one representative term for each topology at each order; other terms can be obtained by cyclic permutation of indices. This simplifies the presentation because the result of the final analysis can also be achieved by simple cyclic permutations of indices. Note that, because of the line-of-sight integration we can not decompose the generating function as a product of three generating functions of single variables.

Introducing the new variable η as before we find that

$$\begin{aligned} C^{\kappa}_{pqr} &= \frac{\langle \eta_s(\gamma_1)^p \eta_s(\gamma_2)^q \eta_s(\gamma_3)^r\rangle_c}{\langle \eta_s(\gamma_1)\eta_s(\gamma_2)\rangle_c \langle \eta_s(\gamma_2)\eta_s(\gamma_3)\rangle_c \langle \eta^2(\gamma)\rangle^{p+q+r-3}_c} \\ &= (\kappa_m)^{p+q+r-2} \frac{\langle \kappa_s(\gamma_1)^p \kappa_s(\gamma_2)^q \kappa_s(\gamma_3)^r\rangle_c}{\langle \kappa_s(\gamma_1)\kappa_s(\gamma_2)\rangle_c \langle \kappa_s(\gamma_2)\kappa_s(\gamma_3)\rangle_c \langle \kappa^2(\gamma)\rangle^{p+q+r-3}_c} \\ &= (\kappa_m)^{p+q+r-2} C^{\eta}_{pqr} \end{aligned} \quad (43)$$

The generating function for the convergence field κ_s can then be written as a summation over different indices:

$$\begin{aligned} {}_3\beta_{\kappa}(y_1,y_2,y_3) &= \sum_{p=1}^{\infty} C^{\eta}_{pqr} \frac{y_1^p}{p!}\frac{y_2^q}{q!}\frac{y_3^r}{r!} \\ &= \int_0^{\chi_s} \frac{r^2(\chi)}{\omega^2(\chi)} d\chi \sum_{p=1}^{\infty} \frac{(-\kappa_m)^{p-1}}{p!} C^{\eta}_{p1} \frac{\kappa^p_{\theta_0}}{\langle \kappa^2_s\rangle^p} \times \frac{\kappa_{\theta_{12}}}{\langle \kappa_s(\gamma_1)\kappa_s(\gamma_2)\rangle} \sum_{q=1}^{\infty} \frac{(-\kappa)^q}{q!} C^{\eta}_{q11} \frac{\kappa^q_{\theta_0}}{\langle \kappa^2_s\rangle^q} \frac{\kappa_{\theta_{23}}}{\langle \kappa_s(\gamma_1)\kappa_s(\gamma_2)\rangle} \\ &\times \sum_{r=1}^{\infty} \frac{(-\kappa_m)^{r-1}}{r!} C^{\eta}_{r1} \frac{\kappa^r_{\theta_0}}{\langle \kappa^2_s\rangle^{2r}} y_3^r \left[\frac{\kappa_{\theta_0}}{\langle \kappa^2_s\rangle}\right]^{-3}. \end{aligned} \quad (44)$$

Making a change of variables from convergence κ_s to reduced convergence η_s we can write

$$\begin{aligned} {}_3\beta_{\eta}(y_1,y_2,y_3) &= \frac{1}{[\kappa_m]^2} \int_0^{\chi_s} d\chi \left[\frac{\kappa_{\theta_{12}}}{\langle \kappa_s(\gamma_1)\kappa_s(\gamma_2)\rangle}\right] \left[\frac{\kappa_{\theta_{23}}}{\langle \kappa_s(\gamma_1)\kappa_s(\gamma_2)\rangle}\right] \left[\frac{\kappa_{\theta_0}}{\langle \kappa^2_s\rangle}\right]^{-3} \\ &\times \mu^{\eta}_1 \left[y_1\kappa_m \frac{\omega(\chi)}{r^2(\chi)} \frac{\kappa_{\theta_0}}{\langle \kappa^2_s\rangle}\right] \mu^{\eta}_2 \left[y_2\kappa_m \frac{\omega(\chi)}{r^2(\chi)} \frac{\kappa_{\theta_0}}{\langle \kappa^2_s\rangle}\right] \mu^{\eta}_1 \left[y_3\kappa_m \frac{\omega(\chi)}{r^2(\chi)} \frac{\kappa_{\theta_0}}{\langle \kappa^2_s\rangle}\right]. \end{aligned} \quad (45)$$

As we mentioned above, it is possible to integrate the above equation (which is derived using only small angle approximation). However, note that due to line-of-sight effects it is no longer possible to separate the cumulant correlators of the convergence field in the same way as can be done for the underlying mass distribution. Using the approximations for the expressions which we have already used to simplify the generating function for two-point cumulant correlators, i.e.

$$\langle \kappa_s(\gamma_i)\kappa_s(\gamma_j)\rangle \approx \frac{1}{2}\chi_s\omega^2(\chi_c)\Big[\frac{d^2k}{(2\pi)^2} \mathrm{P(k)} W^2(kr(\chi_c)\theta_0) \exp[ikr(\chi_c)\theta_{ij}]\Big], \quad (46)$$

we can write

$${}_3\beta_{\eta}(y_1,y_2,y_3) = \mu^{\eta}_1(y_1)\mu^{\eta}_2(y_2)\mu^{\eta}_1(y_3). \quad (47)$$

So at this level of approximation we again obtain a factorization property of the cumulant correlators for the reduced convergence field. Also notice that such an approximation would man that the third order reduced cumulant correlators for convergence field can be related to the corresponding quantity for the underlying mass distribution by

$$C^{\eta}_{p11} = C^{\kappa}_{p11}(-\kappa_m)^p. \quad (48)$$

The three-point joint PDF for the convergence field and the reduced convergence field now can be expressed as

$$\begin{aligned} p^{\kappa}(\kappa_1,\kappa_2,\kappa_3) &= p^{\kappa}(\kappa_1)p^{\kappa}(\kappa_2)p^{\kappa}(\kappa_3)\left[1 + b^{\kappa}(\kappa_1)\xi^{\kappa}_{12}b^{\kappa}(\kappa_2) + b^{\kappa}(\kappa_1)\xi^{\kappa}_{12}\nu^{\kappa}_2(\kappa_2)\xi^{\kappa}_{23}b^{\kappa}(\kappa_3) + \text{cyc.perm.}\right] \\ p^{\eta}(\eta_1,\eta_2,\eta_3) &= p^{\eta}(\eta_1)p^{\eta}(\eta_2)p^{\eta}(\eta_3)\left[1 + b^{\eta}(\eta_1)\xi^{\eta}_{12}b^{\eta}(\eta_2) + b^{\eta}(\eta_1)\xi^{\eta}_{12}\nu^{\eta}_2(\eta_2)\xi^{\eta}_{23}b^{\eta}(\eta_3) + \text{cyc.perm.}\right] \end{aligned} \quad (49)$$

The generating function for the reduced cumulant correlator C^{η}_{p11}, i.e. $\mu^{\eta}_2(y)$ and its associated scaling function $\nu^{\eta}_2(x)$ (see Munshi et al. 1999a,b) can be related by

$$\nu^{\eta}_2(x)h^{\eta}(x) = -\frac{1}{2\pi i}\int_{-i\infty}^{i\infty} dy \mu^{\eta}_2(y)\exp(xy), \quad (50)$$

where the scaling variable x has the same meaning as defined earlier. One can also derive a similar expression for cumulative $\nu^{\eta}_2(>x)$, i.e. $\nu^{\eta}_2(>x)$ beyond a certain threshold (see Munshi, Coles, Melott 1999a,b; Munshi, Melott & Coles 2000; Munshi et al. 1999; Munshi & Melott 1998 for details). Using the fact that $p(\kappa) = p(\eta)/\kappa_m$; $b(\kappa) = b(\eta)/\kappa_m$ and $\xi_{\kappa} = \xi_{\kappa}/\kappa^2_m$ we can finally obtain

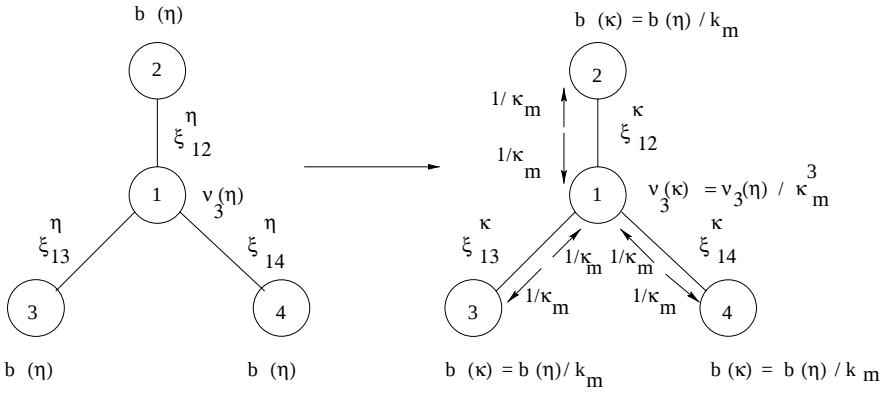

Figure 3. Generating the third order vertex $\nu_3^\kappa(\kappa)$ from its reduced convergence counterpart $\nu_3^\eta(\eta)$. Notice that every link in the η diagram corresponds to an extra factor of $1/\kappa_m^2$ in the κ diagram and hence one of these $1/\kappa_m$ gets attached to one of the two vertices connected by such links. Such a simplification however is possible only after some approximations, as described in the text.

$$\nu_2^\kappa(\kappa) = \frac{\nu_2^\eta(\eta)}{{\kappa_m}^2}. \tag{51}$$

Since the scaling function $\nu_2^\kappa(> x)$ encodes information concerning the skewness of collapsed objects beyond a certain threshold or hot-spots in convergence maps it is interesting to notice how such a quantity is directly related to the three-point cumulant correlators of the background convergence field. We can write the skewness $S_3^\kappa(> \kappa_s)$ of those spots in convergence maps which cross certain threshold κ_s as

$$S_3^\kappa(> \kappa_s) = 3\frac{\nu_2^\kappa(> \kappa_s)}{b^\kappa(> \kappa_s)^2} = 3\frac{\nu_2^\eta(> \eta_s)}{b^\eta(> \eta_s)^2} = S_3^\eta(> \eta_s). \tag{52}$$

It is easy to notice that, independent of cosmology, spots which cross certain threshold η_s in reduced smoothed convergence will have exactly same skewness as the skewness of the overdense regions of the mass distribution $1+\delta = \frac{\rho_s}{\rho_0}$ crossing the same threshold. This is one of the main results in our analysis, in next sections we will show that this results holds good to higher order. Indeed, it turns out that even the PDF of collapsed objects and "hot-spots" in reduced convergence maps will be exactly equal.

5 FOUR-POINT STATISTICS OF COLLAPSED OBJECTS FROM CONVERGENCE MAPS

Four-point cumulant correlators can be analyzed in an exactly similar manner as in the previous section, except that in this case there are two distinct topologies ("snake" and "star" topologies) which make contributions to the correlations. The star topology possesses a completely new vertex of third order, the snake topology (although of same order) is made of lower order tree vertices. Therefore it also provides a unique consistency check of the lower-order diagrams.

The most general four-point cumulant correlator of arbitrary order can be expressed as (Munshi, Melott & Coles 1999a):

$$\begin{aligned}\langle \eta_s^p(\gamma_1)\eta_s^q(\gamma_2)\eta_s^r(\gamma_3)\eta_s^s(\gamma_4)\rangle_c &= \big[C_{p1}^\eta \langle \eta_s(\gamma_1)\eta_s(\gamma_2)\rangle_c C_{q11}^\eta \langle \eta_s(\gamma_2)\eta_s(\gamma_3)\rangle_c C_{r11}^\eta \langle \eta_s(\gamma_3)\eta_s(\gamma_4)\rangle_c C_{s1}^\eta + \text{cyc.perm.} + \ldots \\ &\quad + C_{p1}^\eta \langle \eta_s(\gamma_1)\eta_s(\gamma_2)\rangle_c C_{q1}^\eta \langle \eta_s(\gamma_1)\eta_s(\gamma_3)\rangle_c C_{r1}^\eta \langle \eta_s(\gamma_1)\eta_s(\gamma_4)\rangle_c C_{s111}^\eta + \text{cyc.perm.}\big] \\ &\quad \times \langle \eta_s^2\rangle^{(p+q+r+s-4)}\end{aligned} \tag{53}$$

We will use the same superscript η to denote both the reduced convergence field and the underlying mass distribution. Both fields display similar statistical properties, at least to the level of approximation used here. Developing the four-point function further yields

$$\begin{aligned}\langle \eta_s^p(\gamma_1)\eta_s^q(\gamma_2)\eta_s^r(\gamma_3)\eta_s^s(\gamma_4)\rangle_c &= \int_0^{\chi_s} d\chi \frac{\omega(\chi)^{p+q+r+s}}{r^{2(p+q+r+s-1)}} \big[C_{p1}^\eta \kappa_{\theta_{12}} C_{q11}^\eta \kappa_{\theta_{23}} C_{r11}^\eta \kappa_{\theta_{34}} C_{s1}^\eta + \text{cyc.perm.} \\ &\quad + C_{p1}^\eta \kappa_{\theta 12} C_{q11}^\eta \kappa_{\theta 13}\ C_{r11}^\eta \kappa_{\theta 14} C_{s1}^\eta + \text{cyc.perm.}\big] \kappa_{\theta_0}^{p+q+r+s-4}.\end{aligned} \tag{54}$$

The snake contribution to four-point cumulant correlator can now be written

$$\begin{aligned} C_{pqrs}^{\text{snake}} &= \frac{\langle \kappa_s^p(\gamma_1)\kappa_s^q(\gamma_2)\kappa_s^r(\gamma_3)\kappa_s^s(\gamma_4)\rangle_c^{\text{snake}}}{\langle \kappa_s(\gamma_1)\kappa_s(\gamma_2)\rangle\langle \kappa_s(\gamma_3)\kappa_s(\gamma_4)\rangle\langle \kappa_s^2(\gamma)\rangle^{p+q+r+s-4}} \\ &= \int_0^{\chi_s} d\chi \frac{\omega(\chi)^{p+q+r+s}}{r^{2(p+q+r+s-1)}} C_{p1}^\eta \left[\frac{\kappa_{\theta_{12}}}{\langle \kappa_s(\gamma_1)\kappa_s(\gamma_2)\rangle}\right] C_{q11}^\eta \left[\frac{\kappa_{\theta_{23}}}{\langle \kappa_s(\gamma_2)\kappa_s(\gamma_3)\rangle}\right] C_{r11}^\eta \left[\frac{\kappa_{\theta_{34}}}{\langle \kappa_s(\gamma_3)\kappa_s(\gamma_4)\rangle}\right] C_{s1}^\eta \left[\frac{\kappa_{\theta_0}}{\langle \kappa_s^2\rangle}\right]^{p+q+r+s-4} \end{aligned} \tag{55}$$

Considering the generating function for the snake terms, we obtain the following expression:

$$
\begin{aligned}
{}_4\beta_{\kappa}^{\rm snake}(y_1,y_2,y_3,y_4) &= \sum_{pqrs} C_{pqrs}^{\rm snake}\frac{y_1^p}{p!}\frac{y_2^q}{q!}\frac{y_3^r}{r!}\frac{y_4^s}{s!} \\
&= \frac{1}{[\kappa_m]^2}\int_0^{\chi_s} d\chi\left[\frac{\kappa_{\theta_{12}}}{\langle\kappa_s(\gamma_1)\kappa_s(\gamma_2)\rangle}\right]\left[\frac{\kappa_{\theta_{23}}}{\langle\kappa_s(\gamma_2)\kappa_s(\gamma_3)\rangle}\right]\left[\frac{\kappa_{\theta_{34}}}{\langle\kappa_s(\gamma_3)\kappa_s(\gamma_4)\rangle}\right] \\
&\times\mu_1^{\eta}\left[y_1\frac{\omega(\chi)}{r^2(\chi)}\frac{\kappa_{\theta_0}}{\langle\kappa_s^2\rangle}\right]\mu_2^{\eta}\left[y_2\frac{\omega(\chi)}{r^2(\chi)}\frac{\kappa_{\theta_0}}{\langle\kappa_s^2\rangle}\right]\mu_2^{\eta}\left[y_3\frac{\omega(\chi)}{r^2(\chi)}\frac{\kappa_{\theta_0}}{\langle\kappa_s^2\rangle}\right]\mu_1^{\eta}\left[y_4\frac{\omega(\chi)}{r^2(\chi)}\frac{\kappa_{\theta_0}}{\langle\kappa_s^2\rangle}\right]\left[\frac{\kappa_{\theta_0}}{\langle\kappa_s^2\rangle}\right]^{-4}. \qquad (56)
\end{aligned}
$$

Once again, it is not possible to factorize the generating function because of line-of-sight contributions. After changing variables from κ to η we can write

$$
\begin{aligned}
{}_4\beta_{\eta}^{\rm snake}(y_1,y_2,y_3,y_4) &= \sum_{pqrs} C_{pqrs}^{\rm snake}\frac{y_1^p}{p!}\frac{y_2^q}{q!}\frac{y_3^r}{r!}\frac{y_4^s}{s!} \\
&= \frac{1}{[\kappa_m]^2}\int_0^{\chi_s} d\chi\left[\frac{\kappa_{\theta_{12}}}{\langle\kappa_s(\gamma_1)\kappa_s(\gamma_2)\rangle}\right]\left[\frac{\kappa_{\theta_{23}}}{\langle\kappa_s(\gamma_2)\kappa_s(\gamma_3)\rangle}\right]\left[\frac{\kappa_{\theta_{34}}}{\langle\kappa_s(\gamma_3)\kappa_s(\gamma_4)\rangle}\right] \\
&\times\mu_1^{\eta}\left[\kappa_m y_1\frac{\omega(\chi)}{r^2(\chi)}\frac{\kappa_{\theta_0}}{\langle\kappa_s^2\rangle}\right]\mu_2^{\eta}\left[\kappa_m y_2\frac{\omega(\chi)}{r^2(\chi)}\frac{\kappa_{\theta_0}}{\langle\kappa_s^2\rangle}\right] \\
&\times\mu_2^{\eta}\left[\kappa_m y_3\frac{\omega(\chi)}{r^2(\chi)}\frac{\kappa_{\theta_0}}{\langle\kappa_s^2\rangle}\right]\mu_1^{\eta}\left[\kappa_m y_4\frac{\omega(\chi)}{r^2(\chi)}\frac{\kappa_{\theta_0}}{\langle\kappa_s^2\rangle}\right]\left[\frac{\kappa_{\theta_0}}{\langle\kappa_s^2\rangle}\right]^{-4}. \qquad (57)
\end{aligned}
$$

Similarly, for terms with star topologies, we can write

$$
\begin{aligned}
C_{pqrs}^{\rm star} &= \frac{\langle\kappa_s^p(\gamma_1)\kappa_s^q(\gamma_2)\kappa_s^r(\gamma_3)\kappa_s^s(\gamma_4)\rangle_c^{\rm snake}}{\langle\kappa_s(\gamma_1)\kappa_s(\gamma_2)\rangle\langle\kappa_s(\gamma_3)\kappa_s(\gamma_4)\rangle\langle\kappa_s^2(\gamma)\rangle^{p+q+r+s-4}} \\
&= \int_0^{\chi_s} d\chi\frac{\omega(\chi)^{p+q+r+s}}{r^{2(p+q+r+s-1)}}C_{p111}^{\eta}\left[\frac{\kappa_{\theta_{12}}}{\langle\kappa_s(\gamma_1)\kappa_s(\gamma_2)\rangle}\right]C_{q1}^{\eta}\left[\frac{\kappa_{\theta_{13}}}{\langle\kappa_s(\gamma_1)\kappa_s(\gamma_3)\rangle}\right]C_{r1}^{\eta}\left[\frac{\kappa_{\theta_{14}}}{\langle\kappa_s(\gamma_1)\kappa_s(\gamma_4)\rangle}\right]C_{s1}^{\eta}\left[\frac{\kappa_{\theta_0}}{\langle\kappa_s^2\rangle}\right]^{p+q+r+s-4} \qquad (58)
\end{aligned}
$$

Finally the generating function ${}_4\beta_{\kappa}^{\rm star}(y_1,y_2,y_3,y_4)$ can be written as:

$$
\begin{aligned}
{}_4\beta_{\kappa}^{\rm star}(y_1,y_2,y_3,y_4) &= \frac{1}{[\kappa_m]^2}\int_0^{\chi_s} d\chi\left[\frac{\kappa_{\theta_{12}}}{\langle\kappa_s(\gamma_1)\kappa_s(\gamma_2)\rangle}\right]\left[\frac{\kappa_{\theta_{13}}}{\langle\kappa_s(\gamma_1)\kappa_s(\gamma_3)\rangle}\right]\left[\frac{\kappa_{\theta_{14}}}{\langle\kappa_s(\gamma_1)\kappa_s(\gamma_4)\rangle}\right]\left[\frac{\kappa_{\theta_0}}{\langle\kappa_s^2\rangle}\right]^{-4} \\
&\times\mu_3^{\eta}\left[y_1\frac{\omega(\chi)}{r^2(\chi)}\frac{\kappa_{\theta_0}}{\langle\kappa_s^2\rangle}\right]\mu_1^{\eta}\left[y_2\frac{\omega(\chi)}{r^2(\chi)}\frac{\kappa_{\theta_0}}{\langle\kappa_s^2\rangle}\right]\mu_1^{\eta}\left[y_3\frac{\omega(\chi)}{r^2(\chi)}\frac{\kappa_{\theta_0}}{\langle\kappa_s^2\rangle}\right]\mu_1^{\eta}\left[y_4\frac{\omega(\chi)}{r^2(\chi)}\frac{\kappa_{\theta_0}}{\langle\kappa_s^2\rangle}\right]. \qquad (59)
\end{aligned}
$$

We can now change variables from κ_s to η_s and write:

$$
\begin{aligned}
{}_4\beta_{\eta}^{\rm star}(y_1,y_2,y_3,y_4) &= \frac{1}{[\kappa_m]^2}\int_0^{\chi_s} d\chi\left[\frac{\kappa_{\theta_{12}}}{\langle\kappa_s(\gamma_1)\kappa_s(\gamma_2)\rangle}\right]\left[\frac{\kappa_{\theta_{23}}}{\langle\kappa_s(\gamma_2)\kappa_s(\gamma_3)\rangle}\right]\left[\frac{\kappa_{\theta_{34}}}{\langle\kappa_s(\gamma_3)\kappa_s(\gamma_4)\rangle}\right]\left[\frac{\kappa_{\theta_0}}{\langle\kappa_s^2\rangle}\right]^{-4} \\
&\times\mu_3^{\eta}\left[\kappa_m y_1\frac{\omega(\chi)}{r^2(\chi)}\frac{\kappa_{\theta_0}}{\langle\kappa_s^2\rangle}\right]\mu_1^{\eta}\left[\kappa_m y_2\frac{\omega(\chi)}{r^2(\chi)}\frac{\kappa_{\theta_0}}{\langle\kappa_s^2\rangle}\right]\mu_1^{\eta}\left[\kappa_m y_3\frac{\omega(\chi)}{r^2(\chi)}\frac{\kappa_{\theta_0}}{\langle\kappa_s^2\rangle}\right]\mu_1^{\eta}\left[\kappa_m y_4\frac{\omega(\chi)}{r^2(\chi)}\frac{\kappa_{\theta_0}}{\langle\kappa_s^2\rangle}\right]. \qquad (60)
\end{aligned}
$$

The four-point joint probability distribution function can not be factorized as in the case of underlying mass distribution, but using the same approximation as we have deployed throughout we can simplify these terms and write

$$
\begin{aligned}
{}_4\beta_{\eta}^{\rm snake}(y_1,y_2,y_3,y_4) &= \mu_1^{\eta}(y_1)\mu_2^{\eta}(y_2)\mu_2^{\eta}(y_3)\mu_1^{\eta}(y_4) \\
{}_4\beta_{\eta}^{\rm star}(y_1,y_2,y_3,y_4) &= \mu_3^{\eta}(y_1)\mu_1^{\eta}(y_2)\mu_1^{\eta}(y_3)\mu_1^{\eta}(y_4), \qquad (61)
\end{aligned}
$$

which implies that, as in the lower-order reduced cumulant correlators, we can write

$$
C_{p111}^{\eta} = (\kappa_m)^{p+1}C_{p111}^{\kappa}. \qquad (62)
$$

The joint probability distribution function for the convergence field and the reduced convergence field now can be written

$$
\begin{aligned}
p^{\kappa}(\kappa_1,\kappa_2,\kappa_3,\kappa_4)d\kappa_1 d\kappa_2 d\kappa_3 d\kappa_4 &= p^{\kappa}(\kappa_1)p^{\kappa}(\kappa_2)p^{\kappa}(\kappa_3)p^{\kappa}(\kappa_4)[1+b^{\kappa}(\kappa_1)\xi_{12}^{\kappa}b^{\kappa}(\kappa_2)+\text{cyc.perm.} \\
&+b^{\kappa}(\kappa_1)\xi_{12}^{\kappa}\nu_2^{\kappa}(\kappa_2)\xi_{23}^{\kappa}\nu_2^{\kappa}(\kappa_3)\xi_{34}^{\kappa}b(\kappa_4)+\text{cyc.perm.} \\
&+\nu_1^{\kappa}(\kappa_1)\xi_{14}^{\kappa}b^{\kappa}(\kappa_2)\xi_{24}^{\kappa}b^{\kappa}(\kappa_3)\xi_{34}^{\kappa}b^{\kappa}(\kappa_3)\nu_3^{\kappa}(\kappa_4)+\text{cyc.perm.}]d\kappa_1 d\kappa_2 d\kappa_3 d\kappa_4 \\
p^{\eta}(\eta_1,\eta_2,\eta_3,\kappa_4)d\eta_1 d\eta_2 d\eta_3 d\eta_4 &= p^{\eta}(\eta_1)p^{\eta}(\eta_2)p^{\eta}(\eta_3)p^{\eta}(\eta_4)[1+b^{\eta}(\eta_1)\xi_{12}^{\eta}b^{\eta}(\eta_2)+\text{cyc.perm.} \\
&+b^{\eta}(\eta_1)\xi_{12}^{\eta}\nu_2^{\eta}(\eta_2)\xi_{23}^{\eta}\nu_2^{\eta}(\eta_3)\xi_{34}^{\eta}b^{\eta}(\eta_4)+\text{cyc.perm.} \\
&+\nu_1^{\eta}(\eta_1)\xi_{14}b^{\eta}(\eta_2)\xi_{24}^{\eta}b^{\eta}(\eta_3)\xi_{34}^{\eta}b^{\eta}(\eta_3)\nu_3^{\eta}(\eta_4)+\text{cyc.perm.}]d\eta_1 d\eta_2 d\eta_3 d\eta_4. \qquad (63)
\end{aligned}
$$

The generating function for reduced cumulant correlator C_{p11}, i.e. $\mu_2(y)$ and $\nu_2^{\eta}(x)$ can be related by

$$\nu_3^{\eta}(x)h^{\eta}(x) = -\frac{1}{2\pi i}\int_{-i\infty}^{i\infty} dy\mu_3^{\eta}(y)\exp(xy), \tag{64}$$

where the scaling variable x has the same meaning as defined earlier. One can also derive a similar expression for the cumulative $\nu_3^{\kappa}(>x)$, i.e. $\nu_3^{\eta}(>x)$ beyond a certain threshold; see Munshi et al. (1999a,b,c) for details. Using the fact that $p(\kappa) = p(\eta)/\kappa_m$; $b(\kappa) = b(\eta)/\kappa_m$; $\nu_2(\kappa) = \nu_2(\eta)/\kappa_m$ and $\xi_\kappa = \xi_\eta/\kappa_m^2$ we can finally obtain

$$\nu_3^{\kappa}(\kappa) = \frac{\nu_3^{\eta}(\eta)}{{\kappa_m}^3}. \tag{65}$$

Since the scaling function $\nu_3(>x)$ encodes information on the kurtosis kurtosis of collapsed objects beyond certain threshold, or hot-spots in convergence maps, it is interesting to notice how such a quantity is directly related to the four-point cumulant correlators ("star"-diagrams) of the background convergence field. We can write the kurtosis $S_4(>\kappa_s)$ of those spots in convergence maps which cross certain threshold κ_s as:

$$S_4^{\kappa}(>\kappa_s) = 4\frac{\nu_3^{\kappa}(>\kappa_s)}{b^{\kappa}(>\kappa_s)^3} + 12\frac{\nu_2^{\kappa}(>\kappa_s)^2}{b^{\kappa}(>\kappa_s)^4} = 4\frac{\nu_3^{\eta}(>\eta_s)}{b^{\eta}(>\eta_s)^3} + 12\frac{\nu_2^{\eta}(>\eta_s)^2}{b^{\eta}(>\eta_s)^4}. \tag{66}$$

As in the case of skewness, the kurtosis associated with points which cross certain threshold in convergence map will have precisely identical statistical properties as in the underlying density field.

6 FIVE-POINT STATISTICS OF COLLPASED OBJECTS FROM CONVERGENCE MAPS

The five-point cumulant correlators can be related to the fifth order moments of collapsed objects in a very similar manner to the preceding calculations, so we will simply quote the results of such an analysis in this section. The complication here is that, in addition to having star and snake topologies, there is an additional hybrid topology in this case.

For *star* topologies, the appropriate integrals will involve five node functions. Four of these will be of the form ν_1, and one ν_4. There will also be four links between these nodes denoting the correlations. Hence we can write

$$\begin{aligned}
{}_5\beta_{\kappa}^{\rm star}(y_1,y_2,y_3,y_4,y_5) &= \int_0^{\chi_s} r^2(\chi)d\chi \left[\frac{\kappa_{\theta_{15}}}{\langle\kappa_s(\gamma_1)\kappa_s(\gamma_5)\rangle}\right]\left[\frac{\kappa_{\theta_{25}}}{\langle\kappa_s(\gamma_2)\kappa_s(\gamma_5)\rangle}\right]\left[\frac{\kappa_{\theta_{35}}}{\langle\kappa_s(\gamma_3)\kappa_s(\gamma_5)\rangle}\right]\left[\frac{\kappa_{\theta_{45}}}{\langle\kappa_s(\gamma_4)\kappa_s(\gamma_5)\rangle}\right] \\
&\times \left[\frac{\kappa_{\theta_0}}{\langle\kappa_s^2\rangle}\right]^{-5}\mu_4^{\eta}\left[y_1\frac{\omega(\chi)}{r^2(\chi)}\frac{\kappa_{\theta_0}}{\langle\kappa_s^2\rangle}\right]\mu_1^{\eta}\left[y_2\frac{\omega(\chi)}{r^2(\chi)}\frac{\kappa_{\theta_0}}{\langle\kappa_s^2\rangle}\right]\mu_1^{\eta}\left[y_3\frac{\omega(\chi)}{r^2(\chi)}\frac{\kappa_{\theta_0}}{\langle\kappa_s^2\rangle}\right] \\
&\times\mu_1^{\eta}\left[y_4\frac{\omega(\chi)}{r^2(\chi)}\frac{\kappa_{\theta_0}}{\langle\kappa_s^2\rangle}\right]\mu_1^{\eta}\left[]y_5]\frac{\omega(\chi)}{r^2(\chi)}\frac{\kappa_{\theta_0}}{\langle\kappa_s^2\rangle}\right].
\end{aligned} \tag{67}$$

For a *snake* topology the relevant contributions will come from three generating functions of three-point reduced cumulant correlators C_{p11} denoted as before by $\mu_2(y)$, and two generating function of two-point reduced cumulant correlators C_{p1} which we have denoted by $\mu_1(y)$:

$$\begin{aligned}
{}_5\beta_{\kappa}^{\rm snake}(y_1,y_2,y_3,y_4,y_5) &= \int_0^{\chi_s} r^2(\chi)d\chi \left[\frac{\kappa_{\theta_{12}}}{\langle\kappa_s(\gamma_1)\kappa_s(\gamma_2)\rangle}\right]\left[\frac{\kappa_{\theta_{23}}}{\langle\kappa_s(\gamma_2)\kappa_s(\gamma_3)\rangle}\right]\left[\frac{\kappa_{\theta_{34}}}{\langle\kappa_s(\gamma_3)\kappa_s(\gamma_4)\rangle}\right]\left[\frac{\kappa_{\theta_{45}}}{\langle\kappa_s(\gamma_4)\kappa_s(\gamma_5)\rangle}\right] \\
&\times \left[\frac{\kappa_{\theta_0}}{\langle\kappa_s^2\rangle}\right]^{-5}\mu_1^{\eta}\left[y_1\frac{\omega(\chi)}{r^2(\chi)}\frac{\kappa_{\theta_0}}{\langle\kappa_s^2\rangle}\right]\mu_2^{\eta}\left[y_2\frac{\omega(\chi)}{r^2(\chi)}\frac{\kappa_{\theta_0}}{\langle\kappa_s^2\rangle}\right]\mu_2^{\eta}\left[y_3\frac{\omega(\chi)}{r^2(\chi)}\frac{\kappa_{\theta_0}}{\langle\kappa_s^2\rangle}\right] \\
&\times\mu_2^{\eta}\left[y_4\frac{\omega(\chi)}{r^2(\chi)}\frac{\kappa_{\theta_0}}{\langle\kappa_s^2\rangle}\right]\mu_1^{\eta}\left[y_5\frac{\omega(\chi)}{r^2(\chi)}\frac{\kappa_{\theta_0}}{\langle\kappa_s^2\rangle}\right].
\end{aligned} \tag{68}$$

For the hybrid topology the contributions will come from the generating function of four-point reduced cumulant correlators C_{p111} denoted as before by $\mu_2(y)$, three-point reduced cumulant correlator C_{p11} and the rest of the nodes $\mu_2(y)$ will be generating function for two-point cumulant correlators C_{p1}. So finally we can write

$$\begin{aligned}
{}_5\beta_{\kappa}^{\rm hybrid}(y_1,y_2,y_3,y_4,y_5) &= \int_0^{\chi_s} r^2(\chi)d\chi \left[\frac{\kappa_{\theta_{13}}}{\langle\kappa_s(\gamma_1)\kappa_s(\gamma_3)\rangle}\right]\left[\frac{\kappa_{\theta_{23}}}{\langle\kappa_s(\gamma_2)\kappa_s(\gamma_3)\rangle}\right]\left[\frac{\kappa_{\theta_{34}}}{\langle\kappa_s(\gamma_3)\kappa_s(\gamma_4)\rangle}\right]\left[\frac{\kappa_{\theta_{45}}}{\langle\kappa_s(\gamma_3)\kappa_s(\gamma_4)\rangle}\right] \\
&\times \left[\frac{\kappa_{\theta_0}}{\langle\kappa_s^2\rangle}\right]^{-5}\mu_1^{\eta}\left[y_1\frac{\omega(\chi)}{r^2(\chi)}\frac{\kappa_{\theta_0}}{\langle\kappa_s^2\rangle}\right]\mu_1^{\eta}\left[y_2\frac{\omega(\chi)}{r^2(\chi)}\frac{\kappa_{\theta_0}}{\langle\kappa_s^2\rangle}\right]\mu_3^{\eta}\left[y_3\frac{\omega(\chi)}{r^2(\chi)}\frac{\kappa_{\theta_0}}{\langle\kappa_s^2\rangle}\right] \\
&\times\mu_2^{\eta}\left[y_4\frac{\omega(\chi)}{r^2(\chi)}\frac{\kappa_{\theta_0}}{\langle\kappa_s^2\rangle}\right]\mu_1^{\eta}\left[y_5\frac{\omega(\chi)}{r^2(\chi)}\frac{\kappa_{\theta_0}}{\langle\kappa_s^2\rangle}\right].
\end{aligned} \tag{69}$$

Making a change of variables again from the convergence field κ_s to the reduced convergence field η_s we obtain the following expressions for the five-point generating functions which, again, cannot be factorised. For the star topology we have

$$\beta_{\eta}^{\rm star}(y_1,y_2,y_3,y_4,y_5) = \frac{1}{[\kappa_m]^2}\int_0^{\chi_s} r^2(\chi)d\chi \left[\frac{\kappa_{\theta_{15}}}{\langle\kappa_s(\gamma_1)\kappa_s(\gamma_5)\rangle}\right]\left[\frac{\kappa_{\theta_{25}}}{\langle\kappa_s(\gamma_2)\kappa_s(\gamma_5)\rangle}\right]\left[\frac{\kappa_{\theta_{35}}}{\langle\kappa_s(\gamma_3)\kappa_s(\gamma_5)\rangle}\right]\left[\frac{\kappa_{\theta_{45}}}{\langle\kappa_s(\gamma_4)\kappa_s(\gamma_5)\rangle}\right]$$

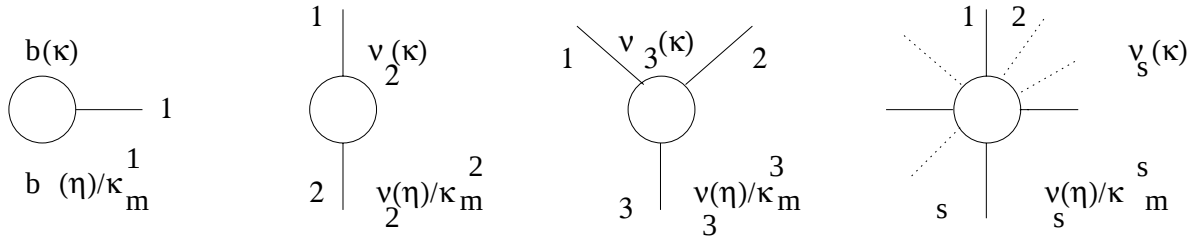

Figure 4. Transformation of nodes representing bright spots in convergence maps for a change of variables from convergence κ_s to reduced convergence η_s. However such a decomposition is possible only under certain simplifying assumption (see text for details).

$$\times \left[\frac{\kappa_{\theta_0}}{\langle\kappa_s^2\rangle}\right]^{-5} \mu_1^\eta\left[\kappa_m y_1 \frac{\omega(\chi)}{r^2(\chi)}\frac{\kappa_{\theta_0}}{\langle\kappa_s^2\rangle}\right]\mu_1^\eta\left[\kappa_m y_2 \frac{\omega(\chi)}{r^2(\chi)}\frac{\kappa_{\theta_0}}{\langle\kappa_s^2\rangle}\right]\mu_1^\eta\left[\kappa_m y_3 \frac{\omega(\chi)}{r^2(\chi)}\frac{\kappa_{\theta_0}}{\langle\kappa_s^2\rangle}\right]$$
$$\times\mu_1^\eta\left[\kappa_m y_4 \frac{\omega(\chi)}{r^2(\chi)}\frac{\kappa_{\theta_0}}{\langle\kappa_s^2\rangle}\right]\mu_4^\eta\left[\kappa_m y_5 \frac{\omega(\chi)}{r^2(\chi)}\frac{\kappa_{\theta_0}}{\langle\kappa_s^2\rangle}\right]. \quad (70)$$

For the snake topology the relevant expression is

$$\begin{aligned}\beta_\eta^{\rm snake}(y_1,y_2,y_3,y_4,y_5) &= \frac{1}{[\kappa_m]^2}\int_0^{\chi_s} r^2(\chi)d\chi\left[\frac{\kappa_{\theta_{12}}}{\langle\kappa_s(\gamma_1)\kappa_s(\gamma_2)\rangle}\right]\left[\frac{\kappa_{\theta_{23}}}{\langle\kappa_s(\gamma_2)\kappa_s(\gamma_3)\rangle}\right]\left[\frac{\kappa_{\theta_{34}}}{\langle\kappa_s(\gamma_3)\kappa_s(\gamma_4)\rangle}\right]\left[\frac{\kappa_{\theta_{45}}}{\langle\kappa_s(\gamma_4)\kappa_s(\gamma_5)\rangle}\right]\\
&\times\left[\frac{\kappa_{\theta_0}}{\langle\kappa_s^2\rangle}\right]^{-5}\mu_1^\eta\left[\kappa_m y_1 \frac{\omega(\chi)}{r^2(\chi)}\frac{\kappa_{\theta_0}}{\langle\kappa_s^2\rangle}\right]\mu_2^\eta\left[\kappa_m y_2 \frac{\omega(\chi)}{r^2(\chi)}\frac{\kappa_{\theta_0}}{\langle\kappa_s^2\rangle}\right]\mu_2^\eta\left[\kappa_m y_3 \frac{\omega(\chi)}{r^2(\chi)}\frac{\kappa_{\theta_0}}{\langle\kappa_s^2\rangle}\right]\\
&\times\mu_2^\eta\left[\kappa_m y_4 \frac{\omega(\chi)}{r^2(\chi)}\frac{\kappa_{\theta_0}}{\langle\kappa_s^2\rangle}\right]\mu_1^\eta\left[\kappa_m y_5 \frac{\omega(\chi)}{r^2(\chi)}\frac{\kappa_{\theta_0}}{\langle\kappa_s^2\rangle}\right], \quad (71)\end{aligned}$$

and similarly for the hybrid topology:

$$\begin{aligned}\beta_\eta^{\rm hybrid}(y_1,y_2,y_3,y_4,y_5) &= \frac{1}{[\kappa_m]^2}\int_0^{\chi_s} r^2(\chi)d\chi\left[\frac{\kappa_{\theta_{13}}}{\langle\kappa_s(\gamma_1)\kappa_s(\gamma_3)\rangle}\right]\left[\frac{\kappa_{\theta_{23}}}{\langle\kappa_s(\gamma_2)\kappa_s(\gamma_3)\rangle}\right]\left[\frac{\kappa_{\theta_{34}}}{\langle\kappa_s(\gamma_3)\kappa_s(\gamma_4)\rangle}\right]\left[\frac{\kappa_{\theta_{45}}}{\langle\kappa_s(\gamma_4)\kappa_s(\gamma_5)\rangle}\right]\\
&\times\left[\frac{\kappa_{\theta_0}}{\langle\kappa_s^2\rangle}\right]^{-5}\mu_1^\eta\left[\kappa_m y_1 \frac{\omega(\chi)}{r^2(\chi)}\frac{\kappa_{\theta_0}}{\langle\kappa_s^2\rangle}\right]\mu_1^\eta\left[\kappa_m y_2 \frac{\omega(\chi)}{r^2(\chi)}\frac{\kappa_{\theta_0}}{\langle\kappa_s^2\rangle}\right]\mu_3^\eta\left[\kappa_m y_3 \frac{\omega(\chi)}{r^2(\chi)}\frac{\kappa_{\theta_0}}{\langle\kappa_s^2\rangle}\right]\\
&\times\mu_2^\eta\left[\kappa_m y_4 \frac{\omega(\chi)}{r^2(\chi)}\frac{\kappa_{\theta_0}}{\langle\kappa_s^2\rangle}\right]\mu_1^\eta\left[\kappa_m y_5 \frac{\omega(\chi)}{r^2(\chi)}\frac{\kappa_{\theta_0}}{\langle\kappa_s^2\rangle}\right]. \quad (72)\end{aligned}$$

Using the same approximations as we have used before for the lower-order cumulants, we can see that the generating function $\nu_4(y)$ and its associated scaling function $\nu_4(x)$ for the reduced convergence field are, once again, exactly the same as the one for underlying mass distribution. This leads to

$$\begin{aligned}{}_5\beta_\eta^{\rm star}(y_1,y_2,y_3,y_4,y_5) &= \mu_1^\eta(y_1)\mu_1^\eta(y_2)\mu_1^\eta(y_3)\mu_4^\eta(y_4)\mu_1^\eta(y_5),\\
{}_5\beta_\eta^{\rm snake}(y_1,y_2,y_3,y_4,y_5) &= \mu_1^\eta(y_1)\mu_2^\eta(y_2)\mu_2^\eta(y_3)\mu_2^\eta(y_4)\mu_1^\eta(y_5),\\
{}_5\beta_\eta^{\rm hybrid}(y_1,y_2,y_3,y_4,y_5) &= \mu_1^\eta(y_1)\mu_1^\eta(y_2)\mu_3^\eta(y_3)\mu_2^\eta(y_4)\mu_1^\eta(y_5). \quad (73)\end{aligned}$$

As in the case of the fourth-order cumulant correlators, these results now can be used to express the five-point joint probability distribution function for both convergence and reduced convergence field. Clearly the new vertex $\mu_4(y)$ and associated scaling function $\nu_4(x)$ (or the analogous $\nu_4(\eta_s)$ or $\nu_4(\kappa_s)$) can be used to express the fifth-order cumulant for collapsed objects:

$$\nu_4^\kappa(\kappa) = \frac{\nu_4^\eta(\eta)}{\kappa_m^4}. \quad (74)$$

Finally the fifth order one-point moment of the collapsed objects is

$$S_5^\kappa(>\kappa_s) = 5\frac{\nu_4^\kappa(>\kappa_s)}{b^\kappa(>\kappa_s)^4} + 60\frac{\nu_3^\kappa(>\kappa_s)\nu_2^\kappa(\kappa_s)^2}{b^\kappa(>\kappa_s)^4} + 60\frac{\nu_2^\kappa(>\kappa_s)^3}{b(>\kappa_s)^4} = 5\frac{\nu_4^\eta(>\eta_s)}{b^\eta(>\eta_s)^4} + 60^\eta\frac{\nu_3^\eta(>\eta_s)\nu_2^\eta(>\eta_s)}{b^\eta(>\eta_s)^4} + 60\frac{\nu_2^\eta(>\eta_s)^3}{b^\eta(>\kappa_s)^4}. \quad (75)$$

7 GENERALIZATION TO ARBITRARY ORDER STATISTICS

Let us now put together what we have learned so far and explain what can be learned about correlations of arbitrary order. If we consider a diagram of arbitrary topology and of arbitrary order it will consist of different kinds of nodes. These nodes will be represented by associated scaling functions $\mu_s(y)$ and act as generating functions for the reduced cumulant correlators of various order $C_{p...1}$. The term will also consist of products of the factors which represent correlation function associated with the links which join these nodes. Products of these terms when integrated along the line of sight direction will provide us the joint generating function of arbitary order for convergence field κ_s:

$$ {}_N\beta_\kappa^{\rm topology}(y_1,\ldots,y_s) = \int r^2(\chi)d\chi \left[\frac{\kappa_{\theta_0}}{\langle\kappa_s^2(\gamma)\rangle}\right]^{-N} \prod_{\rm all\ links\ (i,j)}^{N-1}\left[\frac{\kappa_{\theta\,ij}}{\langle\kappa(\gamma_i)\kappa(\gamma_j)\rangle}\right] \prod_{\rm all\ nodes\ (k)}^{N}\mu_s^\eta\left[y_k\frac{\omega(\chi)}{r^2(\chi)}\frac{\kappa_{\theta_0}}{\langle\kappa_s^2(\gamma)\rangle}\right]. \quad (76) $$

Changing the variables from convergence field κ_s to reduced convergence η_s we can write

$$ {}_N\beta_\eta^{\rm topology}(y_1,\ldots,y_s) = \frac{1}{[\kappa_m]^2}\int r^2(\chi)d\chi \left[\frac{\kappa_{\theta_0}}{\langle\kappa_s^2(\gamma)\rangle}\right]^{-N} \prod_{\rm all\ links\ (i,j)}^{N-1}\left[\frac{\kappa_{\theta\,ij}}{\langle\kappa(\gamma_i)\kappa(\gamma_j)\rangle}\right] \prod_{\rm all\ nodes\ (k)}^{N}\mu_s^\eta\left[y_k\kappa_m\frac{\omega(\chi)}{r^2(\chi)}\frac{\kappa_{\theta_0}}{\langle\kappa_s^2(\gamma)\rangle}\right]. \quad (77) $$

As before, this is the most general expression and includes all other results which we have obtained so far. We want to emphasize that deriving this result we have not used any approximation other than that of small angles and these integrals can be computed numerically to obtain the joint multi-point PDF for convergence fields.

Given a specific model for the underlying mass distribution we can now relate all the multi-point properties of the projected density field to be obtained from weak lensing surveys. However, as we indicated before, with some approximations it is possible to simplify these results still further. This gives us an interesting insight into the statistical nature of the underlying mass distribution:

$$ {}_N\beta_\eta^{\rm topology}(y_1,\ldots,y_s) = \prod_{\rm all\ nodes\ (k)}^{N}\mu_s^\eta[y_k] \quad (78) $$

These approximations have already been tested against the results of high resolution ray tracing experiments (Munshi & Jain 1999a,b; Munshi 1999)which have confirmed that these simplifications indeed reproduce the results in a remarkably accurate way.

The vertices associated with collapsed objects $\mu_n(y)$, can be linked to generating functions for the vertices in the matter correlation hierarchy in a very interesting way. This has been done in an order-by-order expansion (Bernardeau & Schaeffer 1992; Munshi, Coles & Melott 1999a) and also to arbitrary order in a non-perturbative approach (Bernardeau & Schaeffer 1999). These techniques were developed to compute the joint multi-point statistics of collisionless clustering. Our study shows that the statistics of reduced convergence field are deeply linked to the statistics of underlying mass distribution. However, we should keep in mind that although the same functional form for $\nu_n(x)$ holds for both reduced convergence field and the underlying mass distribution the variance associated with them are very different. The variance for the mass distribution is very high on small length scales, while the variance of reduced convergence field is small. This means that while it is possible to compute asymptotic forms for the scaling functions (such as $\nu_n(x)$) for very small variance, complete information about $\nu_n(x)$ can only be obtained by a numerical integrations. This has already been done by Munshi & Jain (1999a), Munshi (2000) for the case of PDF and bias.

8 DISCUSSION

In this paper we have explored the statistics of regions where the lensing convergence exceeds some threshold value. Our main purpose in this is to demonstrate the deep connection between statistical descriptors of the convergence and those of the underlying mass.

Ongoing weak lensing surveys with wide field CCD are likely to produce shear maps on areas of order 10 square degrees or less; existing feasibility studies cover relatively small angles (Bacon et al. 2000; van Waerbeke et al. 2000). In the future, areas larger than $10^\circ \times 10^\circ$ are also feasible, e.g. from the MEGACAM camera on the Canada France Hawaii Telescope and the VLT Survey Telescope. Ongoing optical (SDSS; Stebbins et al. 1997) and radio (FIRST; Refregier et al. 1997) surveys can also provide useful imaging data for weak lensing surveys. Such surveys will provide maps of the projected density of the universe and thus will help us both to test different dark matter models and probe the background geometry of the universe. They will also provide a unique opportunity to test different *ansatze* for gravitational clustering in the highly non-linear regime in an unbiased way. Traditionally such studies have used galaxy surveys, with the disadvantage that galaxies are biased tracers of the underlying mass distribution.

Most previous studies in weak lensing statistics used a perturbative formalism, which is applicable in the quasilinear regime and thus requires large smoothing angles. To reach the quasi-linear regime, survey regions must exceed areas of order 10 square degrees. Since existing CCD cameras typically have diameters of $0.25^\circ - 0.5^\circ$, the initial weak lensing surveys are likely to provide us statistical information on small smoothing angles, of order $10'$ and less. This makes the use of perturbative techniques a serious limitation, as the relevant physical length scales are in the highly nonlinear regime. In our earlier studies

(Munshi & Coles 2000a) we have shown how lower order moments, such as cumulants and cumulant correlators, can also be extended to the case of weak lensing surveys. Although an important step towards understanding the physics of gravitational clustering and constraining the cosmological parameters, this work did not represent a complete picture of the entire PDF and multi-point generalisations of the cumulants and cumulant correlators. This was another aim of the present study. Extending our earlier results we have shown that indeed such results can be obtained once we assume a hierarchical model for the underlying mass distribution.

Numerical comparison of the one point probability distribution function (PDF) and bias of the convergence field have already been carried out by Munshi & Jain (1999a,b). The success of analytical results presented here indicates that the PDF, bias and other higher order statistics for "hot-spots" in convergence maps for a desired cosmological model can be computed as a function of smoothing angle and redshift distribution. Thus physical effects, such as the magnification distribution for Type Ia supernovae, can be conveniently computed. Thus we have a complete analytical description, based on models for gravitational clustering, for the full set of statistics of interest for weak lensing – the one point pdf, two point correlations, and the hierarchy of higher order cumulants and cumulant correlators. This analytical description has powerful applications in making predictions for a variety of models and varying the smoothing angle and redshift distribution of source galaxies; numerical studies are far more limited in the parameter space that can be explored.

The lower-order statistics of "hot-spots" in the convergence field have also already been studied by (Munshi & Jain 1999a,b). They demonstrated that, given a threshold, it is possible to link the statistics of collapsed objects with the 'hot-spots' in convergence field. It was also established that both one-point objects (such as PDF) and two-point objects (such as bias) measured from ray tracing experiments reproduce the analytical predictions with very good accuracy. This strongly motivates this present study, which develops these ideas further. Clearly the hierarchical *ansatz* has not been tested against N-body simulation in its full generality. While we have a very good analytical models for one-point scaling functions (Munshi et al. 1999a,b) which have been tested against numerical simulations, corresponding studies for two-point quantities are still lacking. One expects that situation will improve with availability of larger N-body simulations.

As we found that a suitable transformations of variables from convergence to reduced convergence can make the analysis very simple. Moreover we found that the reduced convergence has exactly the same statistics as the underlying mass distribution under some simplifying assumptions. However, in general the generating functions do not obey a factorization property similar to their counterpart for underlying mass distribution due to a line of sight integration. In general the minimum value of κ i.e. κ_m plays an important role in the transformation.

The dependence of convergence statistics on parameters of the cosmological background model enters through their effect on κ_m. This is why the statistics of η_s are not sensitive to the background geometry or dynamics, but the statistics of convergence κ are very sensitive to parameters such as Ω and Λ. This implies that it is possible to determine or constrain these parameters using weak lensing surveys. Numerical evaluation of this approach has already been done by Munshi & Jain (1999a,b) and Munshi (2000) who found very good agreement between analytical predictions and numerical simulations. While the statistics of the convergence field is very sensitive to the cosmological parameters, the S_N parameters of bright spots which correspond to the collapsed objects in mass distribution are independent of such parameters and are approximately the same as those of collapsed objects; the bias of these bright-spots does depend on cosmplogical parameters.

Our studies also indicate that several approximations involved in weak lensing studies are valid even in the highly non-linear regime of observational interest. While a weakly clustered dark matter distribution is expected to produce small deflections of photon trajectories, it is not clear if the effect of highly over-dense regions capable of producing large deflections can also be modeled using a hierarchical *ansatz* and the weak lensing approximation. Numerical studies have shown that this is indeed the case; the effect of density inhomogeneities on very small angular scales can be predicted with high accuracy using analytical approximations, which confirms for example that the Born approximation is valid in the highly nonlinear regime.

The finite size of weak lensing catalogs will play an important role in the determination of cosmological parameters. It is therefore of interest to incorporate such effects in future analysis. Noise due to the intrinsic ellipticities of lensed galaxies will also need to be modeled. The present study is based on a top-hat window function which is easier to incorporate in analytical computations. It is possible to extend our study to other statistical estimators such as $M_{\rm ap}$, which use a compensated filter to smooth the shear field and may be more suitable for observational studies (Schneider et al 1997; Reblinsky et al 1999). Our method of computing cumulants and cumulant correlators or PDF and bias can also be generalized to the case of other window functions and we hope to present such results elsewhere.

It is interesting to consider an alternative to the hierarchical ansatz for the distribution of dark matter in the highly nonlinear regime. The dark matter can be modelled as belonging to haloes with a mass function given by the Press-Schechter formalism, and spatial distribution modeled as in Mo & White (1996). When supplemented by a radial profile for the dark halos such a prescription can be used to compute the one-point cumulants of the convergence field. Reversing the argument, given the one point cumulants of the convergence field it is possible to estimate the statistics of dark haloes.

Acknowledgment

DM was supported by a Humboldt Fellowship at the Max Planck Institut fur Astrophysik when this work was performed. It is a pleasure for DM to acknowledge many helpful discussions with Francis Bernardeau, Patric Valageas and Katrin Reblinsky. Some of the analytical results which we have presented here were tested successfully against ray tracing simulations in collaboration with Bhuvnesh Jain. It is a pleasure for DM to thank him for several enjoyable collaborations.

REFERENCES

Babul A., Lee M.H., 1991, MNRAS, 250, 407
Bacon D.J., Refregier A., Ellis R.S., 2000, MNRAS, submitted, astro-ph/000308
Balian R., Schaeffer R., 1989, A& A, 220, 1
Bartelmann M., Huss H., Colberg J.M., Jenkins A.
Bernardeau F., 1999, astro-ph/9901117
Bernardeau F., Schaeffer R., 1992, A& A, 255, 1
Bernardeau F., Schaeffer R., 1999, astro-ph/9903087
Bernardeau F., van Waerbeke L., Mellier Y., 1997, A& A, 322, 1
Blandford R.D., Saust A.B., Brainerd T.G., Villumsen J.V., 1991, MNRAS, 251, 600
Boschan P., Szapudi I., Szalay A.S., 1994, ApJS, 93, 65
Colombi S., Bouchet F.R., Schaeffer R., 1995, ApJS, 96, 401
Colombi S., Bouchet F.R., Hernquist L., 1996, ApJ, 465, 14
Couchman H.M.P., Barber A.J., Thomas P.A., 1998, astro-ph/9810063
Davis M., Peebles P.J.E., 1977, ApJS, 34, 425
Fry J.N., 1984, ApJ, 279, 499
Fry J.N., Peebles P.J.E., 1978, ApJ, 221, 19
Groth E., Peebles P.J.E., 1977, ApJ, 217, 385
Gunn J.E., 1967, ApJ, 147, 61
Hamilton A.J.S., Kumar P., Lu E., Matthews A., 1991, ApJ, 374, L1
Hui L., 1999, ApJ, 519, 622
Hui L., Gaztanaga E., 1999, ApJ, 519, 622
Jain B., Mo H.J., White S.D.M., 1995, MNRAS, 276, L25
Jain B., Seljak U., 1997, ApJ, 484, 560
Jain B., Van Waerbeke L., 1999, astro-ph/9910459
Jain B., Seljak U., White S.D.M., 1999, astro-ph/9901191
Jaroszyn'ski M., Park C., Paczynski B., Gott J.R., 1990, ApJ, 365, 22
Jaroszyn'ski M. 1991, MNRAS, 249, 430
Kaiser N., 1992, ApJ, 388, 272
Kaiser N., 1998, ApJ, 498, 26
Limber D.N., 1954, ApJ, 119, 665
Lee M.H., & Paczyn'ski B., 1990, ApJ, 357, 32
Miralda-Escudé J., 1991, ApJ, 380, 1
Mo, H., White, S.D.M., 1996, MNRAS, 282, 347
Munshi D., Bernardeau F., Melott A.L., Schaeffer R., 1999, MNRAS, 303, 433
Munshi D., Melott A.L, 1998, astro-ph/9801011
Munshi D., Coles P., Melott A.L., 1999a, MNRAS, 307, 387
Munshi D., Coles P., Melott A.L., 1999b, MNRAS, 310, 892
Munshi D., Melott A.L., Coles P., 2000, MNRAS, 311, 149
Munshi D., Coles P., 2000a, MNRAS, 313, 148
Munshi D., Coles P., 2000b, MNRAS, in preparation
Munshi D., Jain B., 1999a, MNRAS, submitted, astro-ph/9911502
Munshi D., Jain B., 1999b, MNRAS, submitted,astro-ph/9912330
Munshi D., 2000, MNRAS, submitted, astro-ph/0001240
Mellier Y., 1999, ARA& A, 37, 127
Nityananda R., Padamanabhan T., 1994, MNRAS, 271, 976
Padmanabhan T., Cen R., Ostriker J.P., Summers F.J., 1996, ApJ, 466, 604
Peebles P.J.E., 1980, *The Large Scale Structure of the Universe*. Princeton University Press, Princeton
Peacock J.A., Dodds S.J., 1996, MNRAS, 280, L19
Premadi P., Martel H., Matzner R., 1998, ApJ, 493, 10
Press, W.H., & Schechter, P. 1974, ApJ, 187, 425
Reblinsky, K., Kruse, G.,Jain, B., Schneider, P., astro-ph/9907250
Refregier, A., Brown, S.T., Kamionkowski, M, Cress, C.M., Helfand, D.J., & Babul, A., 1997, AAS Meeting, 191, 83.10
Schneider P., Weiss A., 1988, ApJ, 330,1
Schneider P., van Waerbeke L., Jain B., Kruse G., 1998, MNRAS, 296, 873, 873
Scoccimarro R., Colombi S., Fry J.N., Frieman J.A., Hivon E., Melott A.L., 1998, ApJ, 496, 586
Scoccimarro R., Frieman J., 1999, ApJ, 520, 35
Stebbins A., 1996, astro-ph/9609149
Stebbins A., McKay T., & Frieman J., In proceedings of the 173rd Symposium of the International Astronomical Union, eds. C. S. Kochanek and Jacqueline N. Hewitt, Symposium no. 173, p75
Szapudi I., Colombi S., 1996, ApJ, 470, 131
Szapudi I., Szalay A.S., 1993, ApJ, 408, 43
Szapudi I., Szalay A.S., 1997, ApJ, 481, L1
Szapudi I., Szalay A.S., Boschan P., 1992, ApJ, 390, 350
Valageas, P., 1999a, astro-ph/9904300
Valageas, P., 1999b, astro-ph/9911336
van Waerbeke L., Bernardeau F., Mellier Y., 1999, A& A, 342, 15

van Waerbeke L. et al., 2000, A& A, submitted, astro-ph/0002500
Villumsen J.V., 1996, MNRAS, 281, 369
Wambsganss J., Cen R., Ostriker J.P., 1998, ApJ, 494, 298
Wambsganss J., Cen R., Xu G., Ostriker J.P., 1997, ApJ, 494, 29
Wambsganss J., Cen R., Ostriker J.P., Turner E.L., 1995, Science, 268, 274
Wang Y., 1999, ApJ, in press.